Satellite Technology And Research Centre

STAR@ NUS National University of Singapore

August 10th, 2022, Singapore,

DESIGN OF A TESTBED FOR SATELLITES ATTITUDE CONTROL GROUND EXPERIMENTING

Youness Idlamine
Institut Supérieur de l'Aéronautique et de l'Espace (ISAE-SUPAERO)
Département Conception et Conduite des véhicules
Aéronautiques et Spatiaux (DCAS)
10 Av. Edouard Belin, 31400 Toulouse, France
Email: youness.idlamine@student.isae-supaero.fr

ABSTRACT

Cubesats are the standardized implementation of nano-satellites devised to fill certain missions as bigger satellites but keeping the launching prices low. The ground testing of Cubesats can be approached in several ways, all of them need to reproduce Lower Eart Orbit conditions in terms of low friction, irradiance, and mass distribution. The possible layouts are either based on a moving energy source emulating the sun [1] or a whole moving robotic test bench that also ensures the frictionless environment reproduction [2]. In this paper, a 3-d.o.f. solution is studied and implemented to reproduce the movement of the sun around a cubeSat with the right level of irradiance. The studied solution allows one rotational movement and two translational movements. The only d.o.f. that has an interest on ground testing is the yaw motion-related one. Indeed, the roll and pitch motions are only interesting when we talk about stability of the satellite but for the Sun alignment matters - which is the main subject of study for the attitude control team - these are irrelevant.

NOMENCLATURE

L Light source simulating the Sun.
S Satellite and attached light sensor.
r Distance between L and S.
θ Angle between the normal direction to the sensor plane and the beam direction
r_m Mean distance between L and S.
h_m Mean height of the light source with the ground as reference.
y Distance between L and r_m-radius circle centered on S. $y = r - r_m$
h Height of the light source with the ground as reference.
Φ Irradiance of the light source.
y_M Maximum value for y
θ_M Maximum value for θ
d.o.f. Degree of freedom

INTRODUCTION

The aim of this research-centered project is to devise and assemble a testbed for CubeSats ground testing. The STAR lab I have been working at is designing CubeSats to be launched in lower Earth orbit within 2023 and needs to test their subsystems on the ground. The lab's experiment we were concerned about during these few months is the testing of the proper attitude behavior of the satellite in its different operational phases. To achieve so, there are many requirements and constraints. There are geometrical constraints, time constraints but also cost constraints. In this article, we will show the different design phases, some of the encountered problems and the brought solutions. The solution proposed in this paper could only partly be implemented due to a lack of time and more importantly, to the delays in the shipping time.

REQUIREMENTS SPECIFICATION

For this project, the initial problematic is simple: The labs satellites subsystems need to be tested on the ground before being launched. For that, a testbed is to be designed. To simplify, we draw the initial problem as follows with two main parts: The light source (L) and the satellite sensor (S) as shown in Figure 1

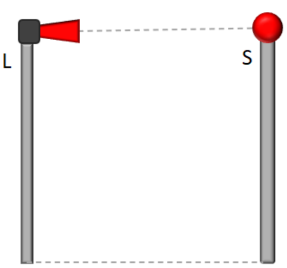

FIGURE 1. Initial configuration

The light source (L) is simulating the Sun's motion around the satellite and is supposed to ensure the mean 1366W/m² irradiance on the light sensor (S) attached to it. To make a complete tracking around the satellite, the degrees of freedom expected by the light source are three in number:

1. Angle between the sensor normal direction and the heat source beam: θ
2. Radial distance to the sensor: r
3. Height of the light source: h

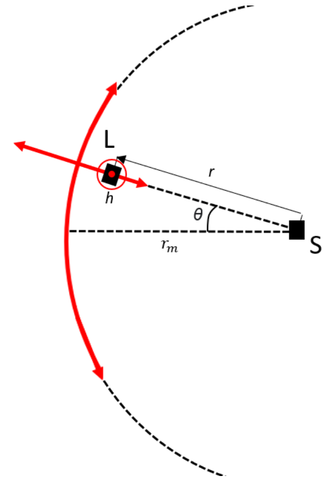

FIGURE 2. Degrees of freedom of the heat source L

These are given in the scheme drawn in Figure 2. Some existing testbeds as that of the AstroFein company [1] provide a 3D tracking but it is not demanded in our case.

CURRENT SOLUTION

The solution used so far for this experiment is based on the simple stand that comes with the light source when purchased (as shown it Figure 3). It is only used to maintain height to a certain value. The first drawback is of course that this configuration is all static and does not allow any motion. It is therefore not possible to operate any tracking around the satellite. Furthermore, the stand has neither great stability nor precision and it can be very easily moved losing its reference frame.

THEORETICAL CONSIDERATIONS

To design the testbed, one should know about the distances, heights and the angles to be achieved to make a Sun-representative tracking. For that, we tested the light source L with a calibrating sensor at different distances from each other and showed that it satisfies the theoretical quadratic luminance-loss law, the light source is being therefore considered consistent for our need. As the capacities of the light source are limited in terms of irradiance, one should choose the right mean radius r_m and radial travel distance around the sensor to get 1366W/m² as mean irradiance value and be able to tune it.

As the first approximation, we suppose there are no losses in the beam and no other source than ours (no reflex-

FIGURE 3. Current testbed

ion, etc). The scene is represented in Figure 4. There are two stations (l and L) and the total heat irradiance flux Φ_l is conserved. The further the L station is, the less energy density the sensor receives on each point of its surface and the evolution is quadratic.
Indeed:

$$\Phi_L = \Phi_l \left(\frac{y}{Y}\right)^2 = \Phi_l \left(\frac{l}{L}\right)^2 \propto L^{-2} \tag{1}$$

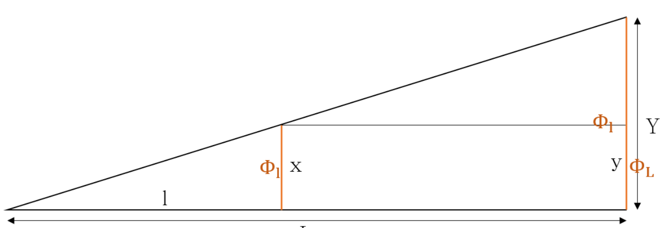

FIGURE 4. Simplified light diffusion sketch

To estimate the accuracy of the measuring device, we tested it through a smaller source of light and it

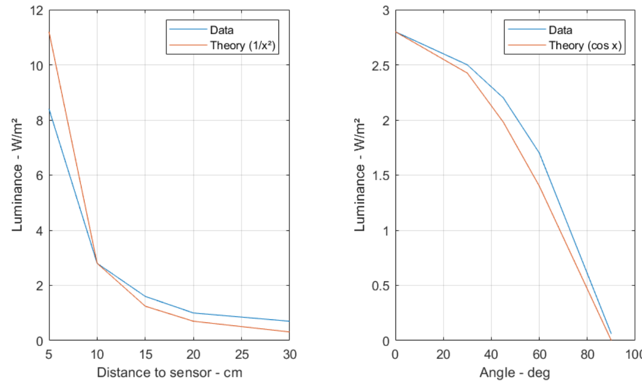

FIGURE 5. Data set comparison with theory

constructively gives - assuming small experimenting errors - the consistent results shown in Figure 5. As expected, the distance to the sensor impacts the luminance by a quadratic factor. For the relative angle between the sensor and the light source, the decreasing shape is cosine-based.

The question we need to answer is about knowing the minimum and maximum distances between the light source L and the sensor S. These will give us the mean radius to consider for the tracking. The used light source is the Joker² 800 HMI Zoom (Figure 6). Following the tests made, it can easily ensure the wanted irradiance if the sensor is placed at more than 3m away which is too much considering the dimensions of the available space for the prototype. After a few tests, it was decided to consider a mean radius of roughly 1.2m centered on the sensor and therefore the light bulb was changed to a mate one to make it less powerful and to enter the wanted range of values, the exact radius value was based on calculations and the markets available components, as it is explained below. A filter was also added to the beamer.

FIGURE 6. Light source

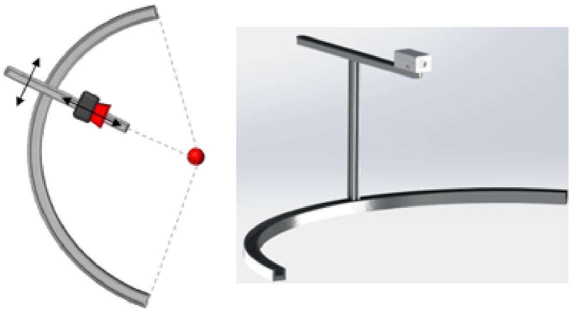

FIGURE 7. Circular configuration sketch

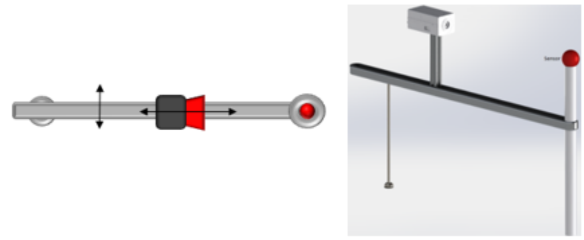

FIGURE 8. Linear configuration sketch

PRELIMINARY IDEAS

Following the requirements specification, three configurations seem to be suited to our need, each of them having pros and cons. At the preliminary ideas step, the geometrical constraints are not taken into consideration and the dimensions are not necessarily at the scale of the version that will be implemented. Also, the shown sketches are only given for visualization matters and no detail is given about the connections between the elements or with the ground.

Circular rack

The first configuration is using a vertical stand that turns around the sensor on a circular rail. The rotational motion is brought by this rack and the linear motion allowing the source to get closer to the sensor is given by an horizontal guide as it can be seen in Figure 7. This solution is the most obvious to think about once we draw the sketch after the requirements specifications. The main advantage is the simplicity of operation of this design. It is very easy to visualize and probably to operate. The second advantage is that the beam, once calibrated correctly for the first time, is always staying centered on the sensor and does not have to be corrected each time, the vertical stand moving along the circular rack. On the other hand, the main drawback of this solution is that it is not compact and will need a lot of space in the lab. Also, the connection between the vertical stand and the ground rack can be hard to handle (regular lubrification, delicate rack-pinion contact, etc).

Linear rack

The second configuration is also using a vertical stand but in this case it is attached to a linear guide connected to the sensor with a ball bearing. The rotational motion is brought by this frictionless bearing and the linear motion allowing the source to get closer to the sensor is given by the horizontal guide. The sketch is drawn in Figure 8. As for the first configuration, this one has its own advantages and drawbacks. The first strength of this solution is its compactness. It is not bulky, and it can be easily moved if necessary without losing its reference frame as it is connected directly to the sensor. The main problem concerns the rigidity of such a configuration. Knowing the length of the horizontal guide (+-1250mm), one can't be sure that the light source will not be moving and thus loose in precision. Finally, this design is not easily reusable and adaptable for any kind of sensor of satellite size. If the design of the vertical stand handling the sensor changes for any convenient reason, the bearing design will need to be done all over again.

Surface plate

The third and last configuration that was discussed is to bring the positioning to the ground level, it is represented in Figure 9. As the irradiance of the sensor depends both on the distance of the light source and on its orientation with the normal direction to the sensor, we can calculate the irradiance in advance for some key positions and thus just place the light source at these positions. We can also tabulate the luminance value at each of these points.

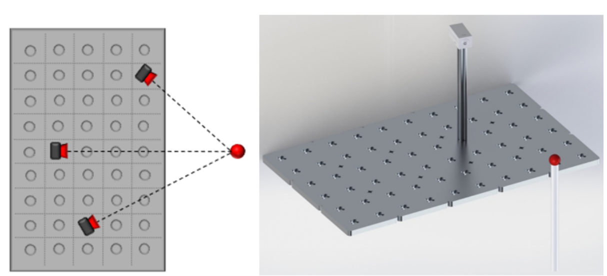

FIGURE 9. Ground configuration sketch

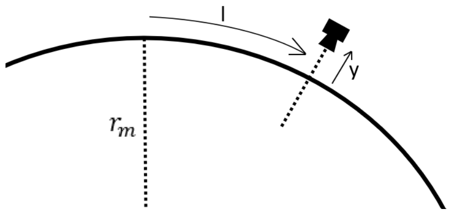

FIGURE 10. Local parameters

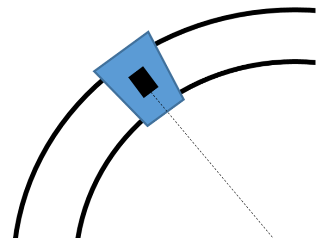

FIGURE 11. Double rail configuration

The main advantage of this solution is the convenience of its usage: the experiment can be very easily operated without any calculation, just reading conversion tables and placing the vertical stand where it needs to be. In addition, ground plates would be easily foldable and only a few squares can be needed. Finally, as for any mechanical system, the less moving parts there are, the more reliable it gets. The main advantage of this system is however its biggest drawback : having a discrete number of possible positionings does not allow any tracking nor any continuous motion of the light source simulating the Sun. Moreover, the light is not sensor-centered and one must ensure its alignment it each time an experiment is done.

DESIGN

We have chosen the **first configuration** because of all the reasons cited above and because it is the solution that opens the most perspectives for future improvements and add-ons. With this configuration, the irradiance depends on both angular and radial positions. Combining the two positioning variables (θ and r), the irradiance can be computed as follows for each position of the flashlight.

$$\Phi_{r,\theta} = \Phi_m \left(\frac{r_m}{r}\right)^2 |cos(\theta)| \tag{2}$$

With Φ_m the irradiance value at the mean position r_m and with a perfect alignment with the sensor ($\theta = 0$). For the experiments, we use local positioning variables based on a scale sticked on the moving parts, we can thus rewrite the formula with the Figure 10 parameters.

$$\Phi_{l,y} = \Phi_m \left(\frac{r_m}{y + r_m}\right)^2 |cos\left(\frac{l}{r_m}\right)| \tag{3}$$

Once the configuration was chosen, the next design step was to define the connection between elements and choose the components to ensure those connections. But before that, we needed to set up a key geometrical vaiables of the configuration: the traveling distances of the moving parts. The travel distances we used for the design is $2y_M = 30cm$ for the radius and 120° for the angular parameter, so $[-60°, +60°]$ and $[r_m - 15cm, r_m + 15cm]$ from the center position using the equation 2 coordinates. This traveling range allowed to change the luminance of a factor f between the maximum luminance position $(0°, r_m - 15cm)$ and the minimum luminance position $(60°, r_m + 15cm)$. For the working radii range, it was not fixed *a priori* but was set following a compromise between the available parts on the market and the luminance range of our light source. Indeed, the parameter f gives an idea of the tuning margin we have by only moving elements position and it strongly depends on the radius r_m:

$$f = \frac{max(\Phi_{r,\theta})}{min(\Phi_{r,\theta})} = \frac{(r_m + y_M)^2}{(r_m - y_M)^2 cos(\theta_M})) \tag{4}$$

First, we drafted a list with the main components. These are: a circular rack, a vertical stand and a linear sliding rack for the radius adjustment. For the fixtures, these needed to be designed once the components were known. The connections we had to have are the following: Ground to circular rack, curved rack to the vertical stand, vertical stand to the horizontal guide and horizontal guide to the light source. The main motion is brought by the curved rack and the solution that ensures less friction combined with easy implementation is the found by *THK Singapore*, a local subsidiary of a Japanese supplier. This part was the starting point of the design as it was the most complex one and the dimensioning of all the others is based on this. Besides, we chose to work with two of these in a concentric configuration to increase the stability of the assembled system. Indeed, as most of the load is concentrated at a certain height of the ground, having twice more ground attachements in the radial and tangential directions was ensuring stability regarding all possible moments. The idea is drafted in Figure 11.

A one rail configuration could have been adopted and would still have kept the system in the right range of allowable moments but it would not bring a great security margin. In the THK's datasheet for the HCR series curved rails [3], the allowable moments are large enough but considering an estimated weight of 8kg placed on top of the vertical stand (including the light source, the radial guide and all third connecting parts) at a mean height h_m of 1m, the system has a moment of inertia of 8kgm² and the balancing moment in radial and tangential directions can therefore wear out the rail and the block and most importantly unalign these. The system would have risked to lose the frictionless aspect we required for the motion fluidity. Furthermore, with only one rail, the ground plate we need for the ground-rail connection would need to be very large to make sure the rail does not come off the ground.

Choice of a tracking radius

In the theoretical considerations section above, we determined by measurements that the mean radius to have a mean luminance of 1366W/m² should be around 1200mm. The idea behind the determination of that mean radius analytically was to use the geometrical scaling margin f as defined above. In other words, for a given power tuning of the light source, we had to choose either the minimum or the maximum value to reach geometrically. As the max luminance value is not easily verifiable using the light sensor we had, we used the minimum luminance and set it to 650 W/m² for the minimum tuning of the light source. From that value of $min(\Phi_{r,\theta})$ and the mean luminance that is required to be 1366W/m² at the center position, we compute the max luminance and thus the scale factor f. Finally, from the scale factor, we can deduce a value for r_m using the equation (4):

$$r_m = y_M \frac{\sqrt{f cos(60°)}+1}{\sqrt{f cos(60°)}-1} = 1280mm \tag{5}$$

The obtained radius validates the measures done at the beginning on the light source. As we use the two rails configuration, the chosen radius must be consistent with what can be found in THK's catalogs. The latter has several radii of the same order of magnitude of what we are looking for: 1000mm;1200mm;1300mm;1500mm. With this mean radius, we can enlighten four working combinations: 1000 and 1300, 1000 and 1500, 1200 and 1300 and finally 1200 and 1500. The chosen rails have a radius of 1000mm and 1300mm, this gives a mean radius r_m of 1150mm. This combination have been chosen because of the rails price,

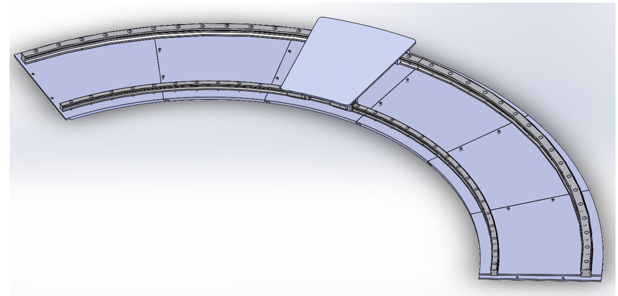

FIGURE 12. Sliding part - assembly

their availability in the country and the shipping times. With this value for r_m, the scale factor f is about **3.38**. The configuration of the system's bottom part with a carriage plate and the right rails is represented in Figure 12. After checking the dimensions of the components provided by THK, we noticed that the two selected rails were not belonging to the same serie, the 1000mmm and the 13000mm were respectively referenced HCR25A1+60/1000R and HCR35A1+60/1300R. The properties not being the same, we had to consider an additional adjusting piece to put over the sliding block of the inner rail to adjust its reference height to the outer one.

Once the main parts were chosen, the vertical and horizontal stands could be selected.The vertical stand has one role to complete, it is to keep all the weight stable at its position and not undergo buckling. For this, a lot of shapes could fit and we selected classical 8-Series Aluminium extrusion with a hollow profile. The main advantage of this component is its high load allowance while being lightweight. It provides and easy connecting method with nuts as well. The nuts ease the connection of aluminium frames with any component using bolts. This part is connected to the carriage plate shown on Figure 12 using L-shaped brackets and M8 bolts. The suppliers can provide all sizes for this part, in steps of 1mm. Considering the assumed minimum operating height of the sensor and the estimated height of all the other components, we chose a height of 650mm for the Aluminium extrusion. The 650mm height corresponds to the minimum sensor height and for any upper height, the light source can be raised manually. The next part to design was the height adjusting mechanism. The first solution drafted was that of a laboratory jack and one was purchased to test its rigidity. This solution was the easiest, the quickest and the cheapest to implement. A lab jack is an easy was to increase or decrease something's height while working on it for convenience, it was provided in several sizes and the purchased one was 200x200m large.

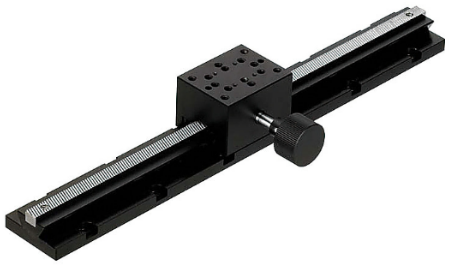

FIGURE 13. Sliding dovetail

Jack problem

The jack is a very interesting solution on paper as it allows large maneuvre while offering a lot of space on the top plate for all remaining parts. In addition, it is not heavy as most of its subparts are in Aluminium. The problem we encountered with this jack is its very limited rigidity when it is deployed. When the jack was at its mean position, the was making the system unstiff and easily movable from its central position. This issue mainly comes from the backlash due to a too high clearance on some parts. Indeed, this jack was not made for the wanted precision. There existed high precision jacks but these only allowed low travel distances. A few things were considered to increase this system's stiffness: adding washers in the high clearanced parts, adding rubber to the moving parts to increase friction in the motion of the subparts or even having tending springs on the four corners of the plate to prevent it from moving. But all of these propositions could not easily solve the problem and we opted for a more adapted part, a dovetail. For the height and radial adjustment mechanisms, we decided to use the same component that will be placed in a different direction. The radial adjustment is done with high precision dovetail using a pinion and rack assembly (Figure 13) found in Misumi's catalog, an international industrial equipment supplier. According to the datasheet, this high precision dovetail slide can allow up to 49N load on a horizontal configuration slide and 25N on a vertical one and travelling on a 30cm distance.

Dovetail disassembly problem

The chosen dovetail is referenced XLONG300 on Misumi's catalog. Once received, we have disassembled the rail and the sliding block part of the assembly to see if it was conceivable for us to link multiple rails together, increasing the travel distance from 30cm to 60cm, for example. That was not a specified requirement but a considered improvement of the system to make it more adaptable. The problem while doing this is that we lost the assembly precision. Indeed, each block was ground fit for precision and shipped after inspection only. This had as consequence to bring more friction to the motion and a too great relative radial effort on the rack teeth. As it is drawn in Figure 14, the effort that allows the motion between the pinion and the rack breaks down in two forces: a tangential force F_t and a radial force F_r. Because of the friction, the radial force became too great and induced bending of the rack. The teeth thus did not remain in contact and the block could not easily be slided using the handle. The way this problem was solved was by putting correctly sized and clearanced 3D-plastic parts under the rail to prevent it from bending and the teeth from jumping. The rail and the block were also lubricated to ease the motion.

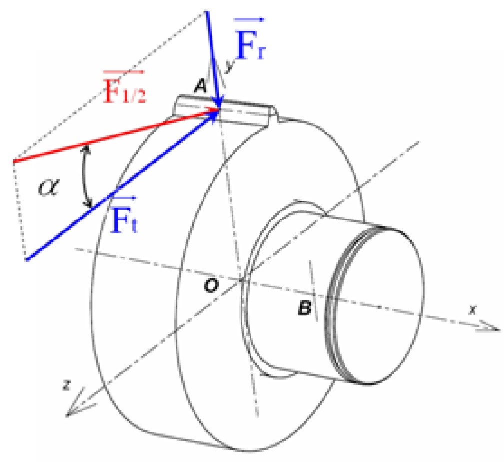

FIGURE 14. Forces on the pinion teeth

The next design step was to design the connecting part between the sliding dovetail and the aluminium extrusion used for the height but also the connecting part between the vertically-positioned dovetail and the radial one. For the first, the requirements were to have two connecting flat surfaces with at least 10 M4 through-all bolts at one side and 4 M8x12 at the other side. For the dovetails connector, the initial solution was very simple: we opted for an L-shaped aluminium part with the right amount of bolts. All the needed bolts and screws are gathered in Table 2.

The last problem we had with the first iteration design was the uncertainty on the flatness of the ground. The ground of the clean room where the prototype will be placed is not controlled and we could have small differences in the reference frame for several points. Considering the height of our system, even a discordance of 0.2mmm between the pea and the trough it could cause a deviation of more than 0.2° from the central position. The most connection points we had with the ground, the less uniform the ground frame became. The damage limiting solution was to only have two external resting edges and make these the same level than worrying about all intermediate points. To that end, we chose to manufacture the ground part in only 2 big 60° plates instead of 6 of 20° each. It is harder to ensure all same-level points in addition to the uncertainty we have on the measures of flatness.

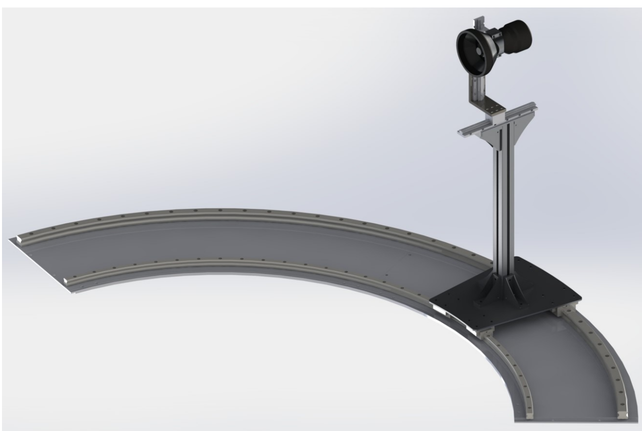

FIGURE 15. First iteration design

The final design for the first iteration is represented in Figure 15 and the components are written down in Table 1. There are 6 different manufactured parts and X buyabale on catalog parts for a total of 26 components and a budget for the buyed parts of roughly 7500S$. To complete this budget and obtain a final estimation of the cost breakdown of the product, one must add the price for the different used screws and the manufactured parts, which is roughly 5150S$. Total cost of the implemented solution is about 12.650S$, or 8500€. The highest delivery time was for the outer guide, which took approximately 65 days to arrive from Japan, it could hence not be assembled to the rest of the system during the present time. The manufactured parts took roughly 4 weeks to be shipped by the usual supplier of the lab. The part we haven't discussed is the light fixture, which connects the vertical dovetail to the Sun. Due to the Sun's particular dimensions, a normal shaft support could not be used and we needed to design one to the right diameter. It is composed by a body part that connects by M4 screws to the vertical dovetail and by a cover part that fixes the Sun's position.

Component	**Features**	**Material**	**Qty**
Inner guide	HCR25A+60/1000R	Carbon steel	2
Outer guide	HCR35A+60/1300R	Carbon steel	2
Vertical stand	Close to 65cm high	A6N01SS-T5	1
Lifting stage	30cm travel	Alu. alloy	1
Brackets	L-shaped	ADC12	6
X-Axis dovetail	30cm travel	Alu. alloy	1
Manufactured			
Ground mounts	2 parts of 60°		6
Carriage plate	24 holes		1
Slider mounts	4 holes	To	2
Top mount	4 M8 threads	be	1
Dovels connector	L-shaped bracket	determined	1
Light fixture	Body: M4		1
	Cover: M6		1

TABLE 1. Components nomenclature

Metric	**Pitch**	**Length**	**Qty**
M4	0.7	$L =$15mm	16
		$L =$20mm	8
		$L =$25mm	4
M6	1	12mm< L <20mm	4
M8	1.25	$L =$10mm	2
		$L =$15mm	16
		$L =$20mm	30
		20mm< L <35mm	8
		40mm< L <45mm	8
M10	1.5	$L =$15mm	2
		$L =$25mm	34
		35mm< L <45mm	8
M12	1.75	$L =$30mm	2
Total: 142			

TABLE 2. Assembly bolts nomenclature

MATERIAL CHOICES

The choice of a material is led in our case by two main factors which are the price and the stress handling. The parts shall not reach ultimate tensile strength or even the plastic deformation limit - yield strength - and shall be as light as possible. The first material we used by default for every manufactured part is 6-series aluminium alloy (6061) which is an alloy of Aluminium, Magnesium and Silicon. The Aluminium combines lightness with sufficient strength properties for most low loading situations. To make it corrosive-resistant, we prefer the manufacturer to anodize the parts into a black color. We used Aluminium alloy for the design and checked with a static simulation if the material fits. In our case, all parts can be manufactured in Aluminium but AISI 304 stainless steel could be used in case of a need for better properties, despite a weight increase.

STATIC STRESS VERIFICATION

Once the first design iteration is done, the objective is to check that parts displacement when assembled is negligible and that we stay in the wanted accuracy margin, meaning less than the manufacturing tolerance (generally 0.1mm). For that, each of the most stress subjected manufactured parts is loaded in Solidworks using a static simulation.

Carriage plate Initial design of this plate was done with a 10mm standard thickness. With 10mm, we are far from UTS and a security margin of more than 50 regarding plastification is obtained. This thickness is therefore oversizing the design and makes the part overweighted. The final thickness of the plate is 5mm. This thickness is sufficient for the stress handling and would not be a problem considering that all the holes are just tapped holes and are not threaded. As a result, with a 5mm carriage plate loaded with roughly 120N, representing the weight, the maximum displacement is at the center and is less than 4.1e-2mm as it can be seen in Figure 16. The displacement can appear huge but the software emphasizes the results with a certain factor to highlight those, the true scale is represented in Figure 17 The maximum reached Von Mises stress is $\sigma_{VM} = 7.2Mpa$ at the bolts and UTS for 6-series aluminium alloys is around 250Mpa. The simulation's results should not be taken as absolutely true because of numerical singularities that could appear during meshing or solving but we can expect the stress to be overall distributed as computed.

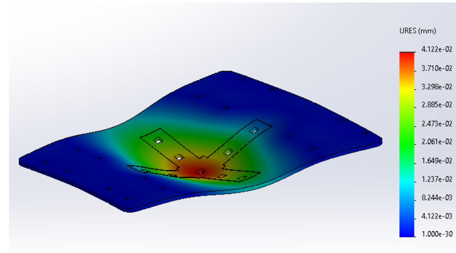

FIGURE 16. Displacement of the carriage plate

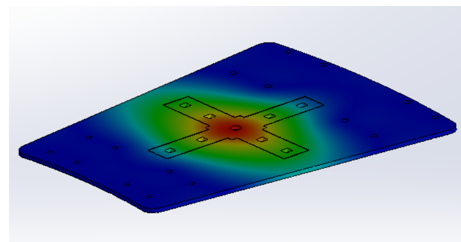

FIGURE 17. Displacement of the carriage plate - True scale

Top mount The objective of the simulation on this component was to see if the M8 bolt we used can handle the stress on two situations. The first simulated case is when the light source is placed at the extremity of the dovel, meaning at the highest distance from the sensor. The second is with a lateral torque which corresponds to the light source placed at r_m and max height. It is important to simulate the latter as the assembly bolts are all aligned along the radial direction, as represented in Figure 18. The two center faces are considered as fixed geometry for the static simulation considering the rigidity of the aluminium frame. As the top mount is not a single part but an assembly, the connections between each subpart had to be specified. For this purpose, a contact connection was set between all components in addition to the bolted connections. On Figure 18, the blue bolt-looking surface is just an emphasized visual representation of the bolts and is not representing the real size of those. For the first simulation, the set force was of the x-dovel weight uniformly distributed all along the mount and the mass of the rest of the components placed at the extremity of the dovel. The results showed that this design was satisfying (see Fig. 19: Maximum reached Von Mises stress around 9.6Mpa and mainly because of the preload on the four bolts. Even though not much visible on the colormap, we can see a little difference in the stress values on the part of the assembly that is the farthest from center, which shows the very small impact of the light source weight on the top mount as the brackets are handling the effort. For the second simulation, a torque was applied. The interest of a torque lies in the fact that it involves the shear stress strength of the bolts. We used this simulation to see is the part is mechanically suited but

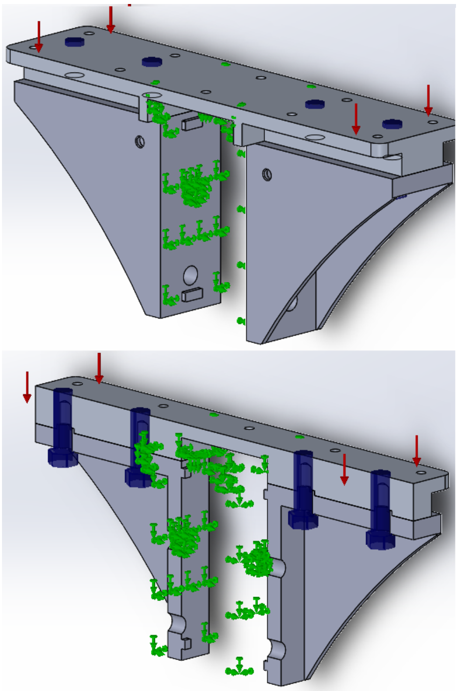

FIGURE 18. Simulation constraints

also to determine whether the M8 metric is sufficient or not. The resulting stresses are not plotted here because these are still very far from allowable limits. The displacements are negligible and the stress distribution is pretty much symmetrical, this shows once again that the weight has no big impact on the top mount strength: the load goes through the bolts and these are correctly designed. It would take a very big accidental force applied on light source to have an impact on this subassembly. Another way to determine if a bolted connection is strong enough for a given load is to do the maths and check whether the bolts can retain the stress. In most cases, including ours, the bolts don't have any stress strength issue as these are made of steel but it can be verified analytically or via standardized tables [4]. For example, the max shear force for non-preloaded bolts can be estimated by:

$$F_{v,Rd} = \frac{\alpha_v f_{ub} A_s}{\gamma_{M_2}} \qquad (6)$$

Where:

- α_v the class factor (0.5/0.6)
- f_{ub} the Ultimate Tensile Strength
- A_s the stressed area for the given metrics ($A_s = 36.6\text{mm}^2$ for standard coarse M8)
- γ_{M_2} the partial factor for bolts (1.25)

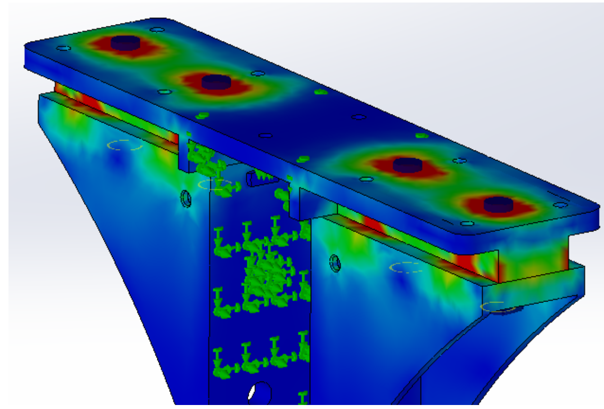

FIGURE 19. Von Mises stress

The exact strength of bolted connections is hard to determine. In most cases, high security margins are adopted to make sure of being far from limits for all kind of stresses. Also, all the empirical coefficients used in the analytical formulas are always overestimated. For high metrics as M8, it is in most cases not needed to worry about strength and stress distribution.

L-bracket The first design of this part is a simple L-shaped 5mm thick Aluminium part. This initial iteration was only satisfying the geometrical constraints and was playing the connection role is was designed for. The purpose of static-simulating it is to highlight the modifications needed for the mechanical strength. After a few iterations, the main modifications that ensure the right strength are: an increased base width, lateral links to shorten the stress flux path on the part, high radius filets to diminish stress concentration and finally a use of AISI304 steel instead of Aluminium alloy (see Fig. 20). A it is discussed in the improvements section, a topology study was also done to highlight the must-keep parts.

ASSEMBLY AND TESTS

The assembly phase in this project is not very substantial because all the parts haven't arrived in the time of the scheduled working weeks. We could only proceed to minor testing of the differents parts separately but not of the whole assembled system. A few points are however important to highlight. First, the part called Top Mount is to be torqued with M8 screws very precisely to avoid any exceeding strain and to comply with the simulations. The next thing to pay attention to for further assembly/disassembly is the radial alignment. Indeed, there can be tolerance errors on each M4 screw hole of the horizontal dovetail these can add up.

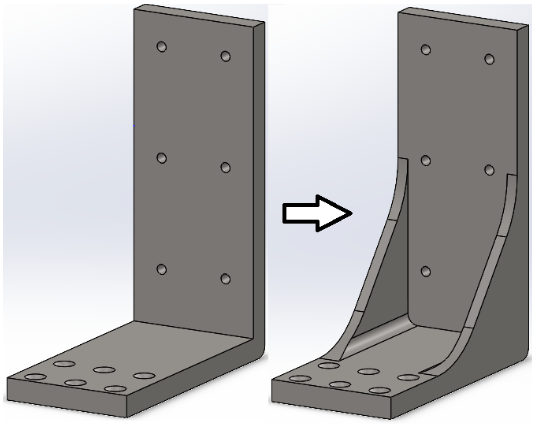

FIGURE 20. Changes on the L-bracket

To illustrate, we made the calculation with a tolerance margin of 0.1mm on two hole rows that are 50mm apart: the misalignment is about 0,22°. If the rows are 250mm apart, the misalignment drops to 0,04°, which is a lot more acceptable. We therefore have every interest in distancing the screwing holes and not use all the 6 screw rows. Finally, for the assembly procedure, the Top mount part shall be mounted to the dovetail before adding the brackets or the M4 screws will be unreachable from bottom.

Alignment issues

The alignment of the components with the satellite is a very complex matter to handle. Indeed, the whole design is based on one supposition: we know where the center of the circle is and we simply need to place the satellite sensor at that position for the experiment to start. But it is in fact very complex to find out where the center position is as there is no physical indicator of it. Geometrically, one can draw two ligns from the extremities of the rail and the intersection would give the center. The problem is that the base of the sensor (Figure 3) is square shaped and makes the center position unreachable. We thought of two solutions based on lasers. One can use 1 laser fixed to the light source but the laser beam would give one locus of the center. The second solution is to use two different lasers. The first one would be at the same level as the light source and the second would be offset by a dozen centimeters in height. Knowing the radius of the circle and the offset, one can compute the angle at which the laser needs to be oriented. The second laser would give the second locus to the center position. This solution is not easy to implement but has the advantage of being the cheapest that works on paper.

SERVICE LIFE

As for all the dynamically sollicited systems, the assembly will be undergoing fatigue and the number of cycles is not illimited, one shall therefore estimate the service life of the assembly. Generally, the most critical parts of a mechanical system are ball bearings and fretted parts because of the friction that can cause pitting or scoring. In our system, the elements to consider for the service life are the parts undergoing dynamic stress. These are mainly the circular rails (inner and outer) and the linear translation dovels used for the radial and z-axis motions. If one knows the correspondance between the different degrees of freedom, it can define a cycle and compute the number of cycles that can be achieved by each part. The service life of the whole system would be hence reduced to the shortest. For the THK guides used for the circular motion, the supplier gives a formula to estimate the number of kilometers that can be acheved by the rails. The latter depends on the working environment and basically the load.

$$L = \left(\frac{f_H f_T f_C}{f_w} \frac{C}{P_C} \right)^3 \cdot 50 \tag{7}$$

With:

- L: Rated life in km
- f_h : Hardness factor
- f_T : Temperature factor
- f_C : Contact factor
- f_w : Load factor
- C : Basic dynamic load rating [N]
- P_C : Calculated load [N]

The hardness factor is equal to 1 for most LM guides as the raceway hardness is between 58 and 60 HRC. As the operating temperature is the ambiant temperature, the temperature factor is also 1. The contact factor intervenes when there are multiple blocks used in close contact to each other. In our case, it is still 1. Finally, the load factor is conidering all the vibrational effects or impacts during the starting and stopping phases, we took it to 1 as the operating speed is very slow. At the end, the formula is simply based on a basic dynamic loading (C) under which the rated life of a group of identical LM Guide units independently operating is 50 km, it is given for each rail reference. For the 1000mm radius railn the service life is $L_{1000} = 2.28\text{e}5$km and for the 1300mm one, it is almost 7 times higher: $L_{1300} = 1.5\text{e}6$km. By dividing the rated life by the effective length of each rail, we estimated the number of complete trackings that could be done. As for the service life L, the achievable number of trackings is big enough. For the x-dovel, the service life depends on many parameters and is not provided by the supplier of this component. However, as for all pinion-rack power transmission, the service life will strongly depend on the used lubricant and whether this lubricant is applied often. In this case, there is not doubt that the service life is exceeding the need.

IMPROVEMENTS

The first design improvement we can think of if reducing the unuseful material. For this aim, we made a preliminary topological study on one of the key parts: the dovels connector. The result of the first analysis (low volumic fraction of material removed) is shown on Figure 21 and it shows where is the material that stress flux goes through. The purpose would be to redesign the part to make it fit the topological but with smoother curves. Indeed, such an irregular shape can not be as easily achieved with metal as with 3D printed plastic.

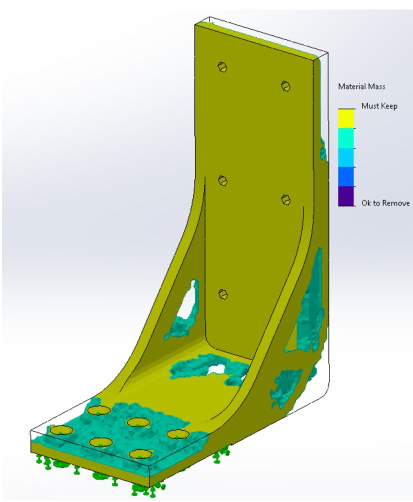

FIGURE 21. First topological analysis result

On this analysis, we imposed to keep a certain depth on the bottom contact surface and a certain thickness around the bolted holes. What appears on this study is that the central area is not sollicited for the force the part is undergoing. Also, the lateral links don't need to be full of matter, the most important part is the furthest from the center. The second improvement we can think of is the anodizing of the parts to avoid corrosion and any light reflexion on silver colored reflexive parts. The supplier could however not ensure it within a reasonable delay. At a loss, in the clean room there is not much humidity so one don't necessarily need the parts to be anodized. Finally, we can add a DC motor to the moving part for an autonomous tracking

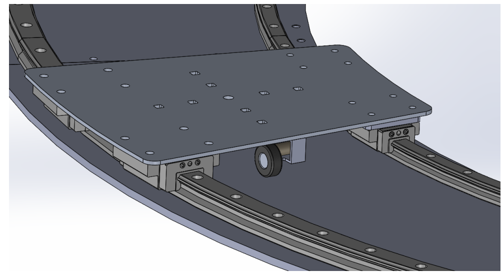

FIGURE 22. Rubber wheel and motor

at a controlled speed and frequency to simulate the sun's behaviour with more accuracy than just sliding it manually (see Fig.22).

CONCLUSION

In closing, the chosen design complies with all the requirements and is satisfying considering the time constraints we had all along the project, it is reliable regarding its service life. We could design a working prototype to be assembled when all parts are delivered. On the personal side, this internship has overall made me learn a lot of things about the research environment even though the project was not a research-only subject. I have been asked to make the experimenting of the satellites easier and the results obtained more reliable by increasing the precision of the testbed and allowing an autonomous tracking system. My job was more that of a research engineer than of a research scientist. Indeed, I have been using my mechanical engineering skills to set up and run the experiment environment for the lab's researchers.

REFERENCES

[1] Raschke, C., de Roemer, S., and Grossekatthoefer, K., 2011. "Test bed for verification of attitude control system".

[2] Gavrilovich, I., Krut, S., Gouttefarde, M., Pierrot, F., and Dusseau, L., 2015. "Robotic test bench for cubesat ground testing: Concept and satellite dynamic parameter identification". In 2015 IEEE/RSJ International Conference on Intelligent Robots and Systems (IROS), pp. 5447–5453.

[3] THK, 2018. *LM Guide, R Guide / Straight-Curved Guide Achieving a Simplified Mechanism. CATALOG No.306-5E.*

[4] Moore, A. M., Rassati, G. A., and Swanson, J. A., 2008. "Evaluation of the current resistance factors for high-strength bolts".